ROLE OF PROXIMITY INTERACTION IN FUSION-FISSION AND RELATED PHENOMENA

A dissertation submitted

For partial fulfilment of the requirement for

The award of the degree of

Masters of Science in

Physics

Under the supervision of

Dr. Manoj Sharma

Submitted by

Rajni

(300904011)

School of Physics and Materials Science

Thapar University

Patiala (147004)

(Punjab) INDIA

July 2011

Dedicated

to

My Mother

CERTIFICATE

This is to certify that the dissertation entitled '**ROLE OF PROXIMITY INTERACTION IN FUSION-FISSION AND RELATED PHENOMENA** 'submitted by MS.RAJNI (Roll no. 300904011) of M.Sc (Physics), Thapar University, Patiala, was carried out by her under our supervision and guidance Dr. Manoj Sharma. I have not submitted this material for credit towards any other degree at Thapar University, Patiala or any other university.

Dr. Manoj Sharma
Associate professor
SPMS, Thapar University
Patiala.

Countersigned By:

Dr. O.P.Pandey
(Prof. & Head)
School of Physics and Materials Science,
Thapar University,
Patiala

Dr. S. K. Mohapatra
Dean of Academic Affairs
Thapar University,
Patiala.

Acknowledgement

First of all, I would like to thank to Dr. Manoj Sharma, my worthy supervisor Associate Professor SPMS, Thapar University, who has been an inspiration during my research work. Without him, this dissertation would not have been possible. I thank him for his patience and encouragement that carried me on through difficult times and for his insight and suggestions that help to shape my research skills.

I also thanks to Dr. O.P.Pandey, Professor and Head, School of Physics and Material science for his support and providing facilities.

A special thanks to Ms. Deepika Jain, research scholar for the help and valuable suggestions whenever I needed out of her busy schedule. I am also thankful to my all classmates for their help and support during the course of this work. I owe my sincere gratitude to my family whose support and obstinate love gave me the energy to complete this dissertation work successfully and also for their untiring help during the difficult moment.

Rajni

ABSTRACT

Proximity interactions have been studied for three channel i.e. $^{64}Ni+^{112,118,124}Sn\rightarrow^{176,182,188}Pt\rightarrow A_1+A_2$. The role of Proximity potential has been studied for above mentioned nuclear reactions using semi classical Extended Thomas Fermi (ETF) approach in SEDF under frozen approximation. Dynamical Cluster Decay (DCM) model is used to investigate the decay pattern whereas ℓ-summed Wong formula has been used for the estimation of fusion excitation functions.

The present work consists of three chapters.

Chapter 1: Introductionary part of all proximity potentials, its different versions and related historical background in reference to fusion-fission dynamics.

Chapter 2: Contains Dynamical cluster Decay Model (DCM), which has been extensively used during last one decade to understand the decay mechanism of nuclear systems formed in heavy ion reactions. In this work we have exploited the advantage of using different Skyrme forces, giving different barriers within one reaction. The dynamical cluster Decay Model (DCM) is a vibrant model which includes the deformation effects of nuclear system and the preformation probability impart much needed nuclear structure information. Wong formula is also discussed in brief.

Chapter 3: Consist of calculations and results. We observe that, the DCM based cross-sections (using GSkI force in proximity interaction) find good comparison with experimental data except at one highest energy, indicating a possibility of competing quasi-fission process at this highest energy. The ℓ-summed Wong formula, with effects of deformation and orientation of nuclei included, fits the fusion cross-sections data exactly for GSkI force, requiring additional barrier modification for SIII Skyrme force.

CONTENTS

Page no.

LIST OF FIGURES

CHAPTER 1

1.1 INTRODUCTION

In the low energy heavy-ion collisions, quasi-elastic scattering and fusion reactions have been studied in recent decades. These studies provide us an ample opportunity to extract the information about the nuclear structure and nucleus-nucleus interaction. One can also explore the mechanism of heavy-ion reactions at near barrier energies. In order to have better understanding of light, heavy and super heavy nuclear systems. Since fusion is a low energy phenomenon, several theoretical models have been developed in recent past at microscopic/macroscopic level and have been robust against vast available experimental data [1-14]. Irrespective of the basis of a theoretical model, one always tries to parameterize the potential in terms of some known quantities like, the charges, masses and isospin of the colliding systems. Various authors have parameterized fusion barriers in terms of these quantities using different approaches. With the availability of different versions of proximity potentials [15], it is of interest to parameterize the fusion barriers using these different versions of proximity potentials and subsequently see it's possible impact in the decay path.

The proximity interaction plays a significant role in addition to coulomb rotational potential. Although the contribution of coulomb and angular momentum dependent interactions have been understood quite Well including the effect of deformations and orientations etc. On these interactions , the choice of nuclear proximity interaction is always a matter of concern and therefore a variety of nuclear proximity potentials is made available as reported in [1-15]. In the present work we focus to understand the role of proximity interaction in reference to formation and decay path of a nuclear system.

When two surfaces approach each other within small distance of 2-3 fm Comparable to the surface thickness of interacting nuclei(as in heavy ion collisions) or when a nucleus is at the verge of dividing itself into two fragments (as in nuclear fission) , then the two surfaces actually face each other across a small gap or crevice. In both the cases, the surface energy term alone (corrected for the curvature effect etc.) could not give rise to the strong attraction that is observed when the two surfaces are brought in close proximity. Such additional forces are called proximity force [1] .

$$V_p = \iint e(D)d\sigma + \text{correction} \qquad (1)$$

this is the proximity energy term associate with curved gap Here e(D) is the interaction energy per unit area of two parallel surfaces at the appropriate separation D. the integration is taken over the gap or crevice area .As there is always a possibility of curvature of surface defining the gap so a correction term is included. It may be note that the gap width D is a slowly varying function of position on the surface. if we define J(D)dD as the area of surface that define two such curve at D and D+dD then eq.(1) may be written as

$$V_P(\text{gap,surf}) = \int e(D)\, J(D)\, dD + \cdots \quad (2)$$

It is worth mentioning that J(D) corresponds to the geometry of gap and therefore the two sides of the gap are rotated, twisted, then J(D) will be accordingly modified. The nuclear proximity interaction is calculated in reference to the proximity theorem. Which state that "the force between two gently curved surfaces in close proximity is proportional to the interaction potential per unit area between the two flat surfaces". This theorem is very useful in contest of proximity interaction in reference to nuclear dynamics and all the proximity potentials are based on this theorem.

There are some models which explain these potential and these model are prox77,prox88,prox00,prox00DP,Bass1973,Bass1977,Bass1980,CW76,BW91,Winther95,Ngo1980,DenisovDP are used extensively to understand the role of nuclear proximity potential in formation of a compound nuclear system.

Different proximity potentials can be written as a product of geometrical factor and universal function Φ(ξ). According to the original version of proximity potential [1], interaction potential between two surfaces can be written as

$$V_N^{prox77}(r) = 4\pi\gamma b\bar{R}\Phi(\xi)\ \text{MeV} \quad (3)$$

Where surface energy coefficient γ_0 taken from the Lysekil mass formula (in MeV= fm^2) is written as:

$$\gamma = \gamma_0\left[1 - k_s\left(\frac{N-Z}{A}\right)^2\right] \quad (4)$$

Here N, Z, and A refer to the combined system of the two interacting nuclei. Here, γ_o=0.9517 MeV fm^2 and k_s = 1:7826. With $\bar{R}$ is the mean curvature radius and Φ(ξ) is the universal function. This proximity potential is popularly known as Prox 77.

With modified mass formula, the values of coefficients γ_o and k_s are 1.2496 MeVfm^2 and 2.3, respectively, showing deeper alteration compared to above coefficients. This potential is marked as Prox 88. In recent years, modifications over original proximity potential have also been suggested. The prime aim behind this modification is to correct the overestimates reported in prox 77 and to account for new data. In the modified version much attention is paid to improve the geometrical factor and surface energy coefficient γ_o. $\Phi(\xi)$ is also modified in Prox 00. So in this way we have different potential/models which improve these coefficients and consequently provide better understanding of nuclear reaction dynamics.

In the different versions of potentials(given by blocki) like Bass 73, Bass 77, Bass 80, and CW 76 one may see that although the form of the radius is different but all these potential are spin independent. The newer versions of Winther (BW 91 and AW95) have incorporated a γ similar to the one used in the Prox 77 potential with a slightly different form. The latest version of Ngˆo (Ngˆo 80) has some isospin dependence in the radius parameter. In most of the potentials, modifications are made either through the surface energy coefficients or via nuclear radii.

Another form of proximity potential based on Skyrme Energy Density Formalism (SEDF) has also been exploited in the nuclear reaction dynamics and related phenomena. The shell model density and Thomas Fermi density distribution have been used extensively in the frame work of SEDF.The energy density formalism defines the nuclear interaction potential as

$$V_N(R) = E(R) - E(\infty)$$

i.e. the nucleus-nucleus interaction potential as a function of separation distance, $V_N(R)$, is the difference of the energy expectation value E of the colliding nuclei that are overlapping (at a finite separation distance R) and are completely separated(at $R=\infty$).

An extended discussion of the proximity forces has been given in ref.[1]

1.2 GENERAL TREATMENT

In the frame work of proximity theorem [1], the geometry of the gently variable gap is specified by first choosing a mean gap surface Γ (a two dimensional surface in space) and then considering normal displacements n_A,n_B, locating the gap, n_A-n_B= D(u,v) being the distance between the two sides Γ_A, Γ_B of the gap. The gap width D(u,v) is a (slowly varying) function of position on the surface r, the position being specified by two coordinates u and v.

Since e(D) is, a function of only one variable D, rather than of the two position variables u and v, the surface integral in Eq. (1) reduces to eq.(2).

However if structure of surface is taken into consideration then,eq.(2) can be written as

$$V_p(\text{gap,surf})=\int e(\text{surf},D)J(\text{gap},D)dD+\ldots, \qquad (5)$$

As regards the geometry of the gap we can illustrate the applications of Eq.(5) by several assumptions about the function D(u,v) and the mean gap surface Γ.

Now if we consider the mean gap surface Γ to be so gently curved that the coordinates u,v on the surface Γ are taken as Cartesian coordinates x,y and the normal coordinate n used to specify the gap (n_A- n_B= D) may be taken as the Cartesian coordinate z, with z_A- z_B= D. If the gap width D(x,y) has a least value D = s at x = y = 0 then its width in the vicinity of this point is given by tailor's expansion

$$\begin{aligned} D(x, y) &= s+ 1/2\ D_{xx}x^2 + 1/2\ D_{yy}\ y^2 + ... \\ &= s+ 1/2\ (x^2 / R_x) + 1/2\ (y^2/ R_y) + ... \end{aligned} \qquad (6)$$

Here D_{XX} and D_{YY} are the second derivatives of D with respect to x and y evaluated at the point of least gap width. The directions of x and y are chosen along the principal axes of the quadratic form D(x,y) and there is no cross term in xy in Eq. (6) .

by changing variables from x, y to ξ , η defined by,

$$\xi= x/(2R_X)^{1/2},\eta=y/(2R_y)^{1/2}$$

D may be written as D = s + ρ^2 , with $\rho^2 = \eta^2 +\xi^2$. The proximity energy can be written as

$$\begin{aligned} V_p(s) = \iint dx\ dy\ e(D) &= 2\left(R_xR_y\right)^{\frac{1}{2}} \iint d\xi\ dn\ e(D) \\ &= 2\left(R_xR_y\right)^{1/2} \int_0^\infty 2\pi\rho\ d\rho\ e(D) \\ &= 2\pi\bar{R} \int_{D=S}^\infty dD\ e(D) \\ &= 2\pi\bar{R}\xi(s) \end{aligned} \qquad (7)$$

The quantity $\bar{R}$ geometric mean of the two principal radii of curvature R_x, R_Y, characterizing the gap D. The reciprocal of $\bar{R}$ is $1/(R_X\ R_y)^{1/2}$, the square root of the invariant Gaussian curvature at x = y = 0 of the surface obtained by plotting D Verses x and y. the negative of the partial derivative of Vp(s) with respect to s gives the force between the two surfaces as a function of the separation degree of freedom

$$F(s) = -\left(\frac{\partial V_P}{\partial s}\right) = 2\pi\bar{R}\, e(s) \qquad (8)$$

This leads to the **Proximity Force Theorem** which has been used extensively in heavy ion physics to impart important information in reference to formation and decay process of nuclear systems.

As all the proximity potentials arise from proximity forces, based on the proximity force theorem. The nuclear part of the interaction potential in different proximity potentials is described as a product of geometrical factor representing the mean curvature of the interacting surfaces and a universal function depending on the separation distance. Therefore proximity theorem is used as an important tool for investigation of problems related to heavy ion interaction and their subsequent decays.

1.3 HISTORICAL BACKGROUND OF NUCLEAR PROXIMITY POTENTIALS

- BASS1973, this model was based on the assumption of Liquid drop model.[3]
- Christensen and Winthe give the another form called as Christensen and Winthe1976 or CW76.[4]
- The next was BASS1977.It drive the nucleon-nucleon potential by using Liquid drop model.[5]
- J. Blocki, J. Randrup, W. J. S´wia¸tecki, and C. F. Tsang, gave the another version of proximity potential and this is called as original version of proximity potential and termed as prox77.[1]
- BASS 1977 model was improve by Bass and this model is termed as BASS1980.[7]
- NGO1980 was another form.it was given by H. Ngˆo and Ch. Ngˆo[9]
- Then proximity potential modified by MOLLER & NIX ,they were the two scientist who modified previous form(prox77) of proximity potential & give prox88.the name prox88 comes because it was modified in 1988.[6]
- The refind form of Bass80 potential given by Broglia andWinther known as Broglia andWinther 1991or BW91.[7]
- The another form was given by Aage Winther and known as Aage Winther95.[10]
- The proximity potential again modified by two scientist Mayers & Swiaecki.it is known as proximity 2000 or prox00.[8]

- The next modified form was “modified proximity2000”orprox00DP.it was modified by Royer and Rousseau.[14]
- New Denisov Potential (Denisov DP) was the form given by Denisov.[2]

  One may conclude that variety of nuclear proximity potentials are available and a sincere effort is required to summarize their respective utility in reference to heavy ion physics.

1.4 DIFFERENT KIND OF MODLES & PROXIMITY POTENTIALS FORMALISM:-

We present the details of various proximity potentials used for the Calculation of fusion barriers. Various versions of these Potentials take care of different aspects including the isospin Dependence. In the following, we discuss each of them in brief.

1. Bass 1973 (Bass73):--

This model is based on the assumption of liquid-drop model [3]. Here change in the surface energy of two fragments due to their mutual separation is represented by exponential factor. By multiply with geometrical arguments, one can obtained the nuclear part of the interaction potential as

$$V_N(r)^{Bass73} = -\frac{d}{R_{12}} a_s A_1^{1/3} A_2^{1/3} \exp\left(-\frac{r-R_{12}}{d}\right) \text{MeV} \qquad (1)$$

With $R_{12}=r_o(A_1^{1/3}+A_2^{1/3})$, d=1.35fm, a_s=17.0Mev. The cut-off distance R_{12}=1.35fm is chosen to yield saturation density in the overlap region and r_o=1.07 fm corresponding half of the maximum density for individual nucleus. this potential is labelled as Bass 73.

2. Christensen and Winther 1976 (CW 76):--

Christensen and Winther [4] derived the nucleus-nucleus interaction potential by analyzing the heavy-ion elastic scattering data, based on the semi classical arguments and the recognition that optical-model analysis of elastic scattering determines the real part of the interaction potential only in the vicinity of a characteristic distance. The nuclear part of the empirical potential due to Christensen and Winther is written as

$$V_N^{CW76}(r) = -50\frac{R_1 R_2}{R_1+R_2}\Phi(r-R_1-R_2)\,\text{MeV} \qquad (2)$$

This form of the geometrical factor is similar to that of Bass77.they uses the different radius parameter

$$R_i = 1.233A_i^{1/3} - 0.978A_i^{-1/3}\ \text{fm} \qquad \text{(i=1,2)}$$

The universal function $\Phi(s = r - R_1 - R_2)$ has the following Form

$$\Phi(s) = \exp[-(r - R_1 - R_2/0.63)] \qquad (3)$$

This model is labelled as CW76.

3. Bass 1977(Bass77):--

In this model, nucleus-nucleus potential is derived from the information based on the experimental fusion cross sections by using the liquid drop model and general geometrical arguments. The nuclear part of the potential (for spherical nuclei with frozen densities) can be written as [5]

$$V_N(r)^{Bass77} = -4\pi\gamma \frac{R_1 R_2}{R_1 + R_2} f(r - R_1 - R_2)$$

$$= -\frac{R_1 R_2}{R_1 + R_2} \Phi(r - R_1 - R_2)\ \text{MeV},$$

$$\frac{df}{ds} = -1, \text{ for s=0} \qquad (4)$$

Note that $f(s = r - R_1 - R_2)$ and $\Phi(s = r - R_1 - R_2)$ are the universal functions. Here radius R_i is written as $R_i = (1.16A_1^{1/3} - 1.39A_2^{-1/3})$fm $(i = 1, 2)$ (5)

The form of the universal function $\Phi(s)$ reads as

$$\Phi(s) = [A\exp(s/d_1) + B\exp(s/d_2)]^{-1} \qquad (6)$$

This model was very successful in explaining the barrier heights, positions, and cross sections over a wide range of incident energies and masses of colliding nuclei. This potential is labelled as Bass 77.

4. PROXIMITY 1977(PROX77):--

According to the original version of proximity potential 1977 [1], the interaction potential $V_N(r)$ between two surfaces can be written as:

$$V_N(r) = 4\pi\gamma b\bar{R}\Phi\left(\frac{r - C_1 - C_2}{b}\right)\text{MeV} \qquad (7)$$

In this, the mean curvature radius $\bar{R}$, has the form

$$\bar{R} = \frac{C_1 C_2}{C_1 + C_2},$$

Here

$$C_i = R_i\left[1 - \left(\frac{b}{R_i}\right)^2 + \cdots\cdots\right],$$

R_i , effective sharp radius, given as

$$R_i = 1.28A_i^{1/3} - 0.76 + 0.8A_i^{-1/3}\text{fm} \quad (i=1,2).$$

In Eq. (7) $\Phi(\xi = r - C_1 - C_2/b)$ is a universal function that depends on the separation between the surfaces of two colliding nuclei only.

As these factors do not depend on the isospin content. However γ, the surface energy coefficient, depends on the neutron/proton excess as

$$\gamma=\gamma_0(1-k_s[(N-Z)/N+Z)]^{1/2}) \qquad (8)$$

Where *N* and *Z* are the total number of neutrons and protons. In the present version, $\gamma_o$and k_s were taken to be 0.9517 MeV/fm^2 and 1.7826, respectively. Note that for the symmetric colliding pair, i.e., (*N* = *Z*), $\gamma = \gamma_o$ = 0.9517 MeV/fm^2. If the (N−Z /N+Z) ratio is 0.5, γ reduces to 0.5276 MeV/fm^2. Defining asymmetry parameter $A_s=[N_1+N_2-(Z_1+Z_2)$ $N_1+N_2+(Z_1+Z_2)$]. most of the modified proximity type potentials use different values of the parameter γ[7,8].

The surface width *b* has been evaluated close to unity. Using the above form, one can calculate the nuclear part of the interaction potential $V_N(r)$. This model is referred to as Prox 77 and the corresponding potential as $V_N^{77\text{Prox}}(r)$.

5. Bass 1980 (Bass 80):--

The BASS77 potential form was further improved by Bass[7]. Here $\Phi(s = r - R_1 - R_2)$ is given as:

$$\Phi(s) = [0.033 \exp(s/3.5) + 0.007 \exp(s/0.65)]^{-1}$$

with central radius, R_i, as

$$R_i = R_s\left(1 - \frac{0.98}{R_s^2}\right) \quad (i = 1,2),$$

Where R_i is same as using ref.[15] This potential is labelled as Bass80.

6. Ngˆo 1980 (Ngˆo 80):--

Now BW91 potential was improved by H. Ngˆo and Ch. Ngˆo [9] by using a Fermi-density distribution for nuclear densities as

$$\rho_{n,P}(r) = \frac{\rho_{n,P}(0)}{1 + \exp\left[\left(r - C_{n,P}\right) / 0.55\right]}$$

Where $C_{n,p}$ represent the central radius same as in prox77.here $\rho_{n,p}(0)$ is written as

$$\rho_n(0) = \frac{3}{4\pi}\frac{N}{A}\frac{1}{r_{0_n}^3}\ ; \qquad \rho_p(0) = \frac{3}{4\pi}\frac{Z}{A}\frac{1}{r_{0_p}^3}.$$

They again using the different values of different functions . The universal function $\Phi(s = r - C_1 - C_2)$ (inMeV/fm) is noted by

$$\Phi(s) = \begin{cases} -33 + 5.4(s - s_0)^2, & \text{for } s < s_0, \\ -33\exp\left[-\frac{1}{5}(s - s_0)^2\right], & \text{for } s \geq s_0, \end{cases} \qquad (9)$$

This potential is labelled as Ngo80.

7. PROXIMITY 88(PROX88):--

In this version, using the more refined mass formula due toM¨oller and Nix [6], the value of coefficients γ_o and k_s were modified the value of the coefficient γ & k_s were modified yielding the value = 1.2496MeV/fm^2 and 2.3, respectively. With modified mass formula, the values of coefficients γ_o and k_s respectively, showing deeper alteration compared to above coefficients (used in prox77).

So by using more refind mass formula due to moller & nix. Residrof [7], this is marked as "proximity 1988". In this set of coefficient give stronger than above set (prox77) and called as prox88.

8. Broglia andWinther 1991 (BW 91):--

A refined version of the CW76 potential was derived by Broglia and Winther [7] by taking Woods-Saxon parametrization. This refined potential resulted in

$$V_N^{BW91}(r) = -\frac{V_0}{1+\exp\left(\frac{r-R_0}{0.63}\right)} MeV;$$

With $V_o = 16\pi \frac{R_1 R_2}{R_1 + R_2} \gamma a,$ (10)

by using different value of R & a. We get another modified form of surface energy term γ with slightly difference value as in prox77

$$\gamma = \gamma_o \left[1 - k_s \left(\frac{N_P - Z_P}{A_P}\right)\left(\frac{N_t - Z_t}{A_t}\right)\right],$$

Where γ_o = 0.95 MeV/fm^2 and k_s = 1.8. Note that the second term used in this potential gives different results when the projectile is symmetric ($N = Z$) and the target is asymmetric ($N > Z$). The radius used in this potential has same form like that of Bass with different constants. This potential is labelled as BW 91.

9. Age winther(AW95):--

Winther adjusted the parameters of the above potential through an extensive comparison with experimental data for heavy-ion elastic scattering. This refined adjustment to slight different values of "a" and R_i as [10]

$$a = \left[\frac{1}{1.17\left(1+0.53\left(A_1^{-1/3}+A_2^{-1/3}\right)\right)}\right] \text{fm}$$

And $R_i = 1.20A_i^{1/3} - 0.09$ fm (i=1,2).

Here $R_i=R_1+R_2$ and This potential is labelled as AW95.

10. Proximity 2000(prox00):--

Myers and S´wia¸tecki [8] modified Eq. (7) by using up-to-date knowledge of nuclear radii and surface tension coefficients using their droplet model concept. The prime aim behind this attempt was to remove discrepancy of

the order of 4% reported between the results of Prox 77 .Using the droplet model [11], matter radius was calculated as

$$C_i = c_i+(N_i/A_i)t_i \quad (i = 1, 2), \qquad (11)$$

where c_i denotes the half-density radii of the charge distribution and t_i is the neutron skin of the nucleus. To calculate $c_{i,}$ these authors [8] used two-parameter Fermi function values given in Ref. [12].

By using the value of nuclear charge radius R_{00} (Ref.(13)),The half-density radius, c_i, is obtained as

$$c_i = R_{00i}\left(1 - \frac{7}{2}\frac{b^2}{R_{00i}^2} - \frac{49}{8}\frac{b^4}{R_{00i}^4}\ldots\ldots\ldots\right) \quad (i = 1,2).$$

By using the value of neutron skin [ref. (15)].The nuclear surface energy coefficient γ in terms of neutron skin was given as

$$\gamma = 1/4\pi r_0^2\,[18.63(\text{MeV}) - Q\,(t_1^2 + t_2^2)/2\gamma_0^2]$$

Where t_1 & t_2 are calculated using eq. Given in ref. (15). The value of universal function is obtain as

$$\Phi(\xi) = \begin{cases} -0.1353 + \sum_{n=0}^{5}\left[\frac{c_n}{n+1}\right](2.5-\xi)^{n+1}, & \text{for } 0 < \xi \le 2.5, \\ -0.09551\exp[(2.75-\xi)/0.7176], & \text{for } \xi \ge 2.5. \end{cases} \quad (12)$$

This potential is labelled as Prox 00.

11. Modified proximity 2000(Prox00DP):--

In this proximity model two scientists modified nuclear charge radius R_{00i} by slightly different constants.

$$R_{00i} = 1.2332A_i^{1/3}\left[1 + \frac{2.348443}{A_i} - 0.151541\left(\frac{A_i - 2Z_i}{A_i}\right)\right] \text{ fm} \quad (13)$$

Where (i=1,2)

The above formula is mainly improved by adding the Coulomb diffuseness correction or the charge exchange correction to the mass formulas [14].We implement this radius in the proximity 2000 version instead of the form given in the proximity 2000. This new version of the proximity potential is labelled as Prox 00DP.

12. New Denisov Potential (Denisov DP):--

Denisov [2] performed numerical calculations and parametrized the potential based on 7140 pair within semimicroscopic approximation. In total, 119 spherical or near spherical nuclei along the β-stability line from 16O to 212Po were taken. The potential is evaluated for any nucleus-nucleus combinations at 15 distances between ions around the touching point. By using this database, a simple analytical expression for the nuclear part of the interaction potential $V_N(r)$ between two spherical nuclei is presented as

$V_N(r) = -1.989843[R_1R_2/R_1+R_2]\Phi(r-R_1-R_2-2.652.65)$

$[1+0.003525139[A_2/A_1+A_2/A_1]-0.4113263(I_1+I_2)]$

With

$$I_i = \frac{N_i - Z_i}{A_i} \ (i = 1,2).$$

The effective radii R_i is given as

$$R_i = R_{ip}\left(1 - \frac{3.413817}{R_{ip}^2}\right) + 1.284589\left(I_i - \frac{0.4A_i}{A_i + 200}\right)(i = 1,2),$$

Where proton radius R_{ip} is given by,

$$R_{00i} = \sqrt{\frac{5}{3}}\langle r^2\rangle^{1/2}$$

$$= 1.240A_i^{1/3}\left\{1 + \frac{1.646}{A_i} - 0.191\left(\frac{A_i - 2Z_i}{A_i}\right)\right\} fm \qquad (14)$$

Where (i=1,2) and $\Phi(s=R_1-R_2-2.65)$ is given by the following complex form

$$\Phi(s) = \begin{cases} 1 - s/0.7881663 + 1.229218s^2 - 0.2234277s^3 \\ -0.10138769s^4 - \frac{R_1R_2}{R_1+R_2}(0.184935s^2 + 0.07570101s^3) \\ +(I_1+I_2)(0.0470645s^2 + 0{,}03346870s^3), \\ \text{for} \quad -5.65 \le s \le 0, \\ \left[1 - s^2\left[\begin{matrix}0.05410106\frac{R_1R_2}{R_1+R_2}\exp\left(-\frac{s}{1.760580}\right)\\ -0.5395420(I_1+I_2)\exp\left(-\frac{s}{2.424408}\right)\end{matrix}\right]\right] \\ \times \exp\left(-\frac{s}{0.7881663}\right), \\ \text{for} \quad s \ge 0. \end{cases} \qquad (15)$$

This potential is termed as Denisov DP.

Beside this EDF based proximity potential has also been used extensively in the problems related to heavy ion collisions. The details of EDF base proximity potential are given in chapter 2.

In a recent study [15], all kind of reactions involving symmetric ($N = Z$; $A_1 = A_2$) as well as asymmetric nuclei ($N >> Z$; $A_1 << A_2$) were considered. Barrier positions were parameterized in terms of surface distance $S_B = R_B - C_1 - C_2$. As S_B reduces with mass of the system indicating deeper penetration is needed for heavier nuclei. By adding radii of two nuclei, one can compare the fusion barrier. All proximity potentials follow exponential parametrization [15]

$$S_B = a \exp\left[-b(x-2)^{\frac{1}{4}}\right] \quad (16)$$

Where a and b are the constants having different values for different proximity potentials. The quality of this parameterized fusion position can be judged by analyzing the percentage deviation defined as

$$\Delta R_B\ \% = \frac{R_B^{anal} - R_B^{exact}}{R_B^{exact}} \times 100 \quad (17)$$

The $\Delta R_B\%$ verses Z_1 Z_2variation reported in [15] indicated that in all the three cases(prox77,prox88,prox00), the analytical parameterized forms give good results within in $\approx \pm 1\%$ Further, they also parameterized the fusion barrier heights V_B as

$$V_B = \alpha\left[\frac{1.44 \cdot Z_1 \cdot Z_2}{R_B^{anal}}\left(1 - \frac{1}{R_B^{anal}}\right)\right] \quad (18)$$

Here α is a constant having different values for different proximity potentials. The second term in the above relation takes care of the deviations at lower tail of the fusion barrier heights. Again, the quality of the analytical parametrization is tested [15] where percentage difference between exact and analytical values is in $\approx \pm 1\%$.

In these different versions of potentials like Bass 73, Bass 77, Bass 80, and CW76 one may see that although the form of the radius is different but it is still isospin independent. Further, the corresponding universal functions are also isospin independent. The newer versions of Winther (BW 91 and AW95) have incorporated a γ similar to the one used in the Prox 77 potential with a slightly different form. The latest version of Ngˆo (Ngˆo 80) has some isospin dependence in the radius parameter. In most of the above-mentioned potentials, modifications are made either through the surface energy coefficients or via nuclear radii. One may note that the nuclear part of the potential becomes more s hallow with asymmetry of the reaction. On the other hand, a detailed comparison of different potentials does not show any preference

for the isospin-dependent potential. All models can explain the fusion barrier heights within ±10% and potentials from Prox 88, Bass 80, AW 95, and Denisov DP perform better than others [15]. The fusion cross sections are nicely explained by Bass 80, AW95, and Denisov DP potentials at below as well as above barrier energies.

In the present work we intend to see the role of proximity forces in reference to the decay of hot and rotating nuclear system formed in heavy ion reaction using well known dynamical cluster decay model (DCM), which carries distinct advantage over competing statistical models as the possible decay path is evaporation residue (ER), intermediate mass fragment (IMF) and fusion, fission(FF) etc. In other words ER, IMF and FF can be worked out within one formalism on equal footing. Beside this the important structure effects are also included via preformation probability in the frame work of DCM .

REFERENCES

[1] J. Blocki, J. Randrup, W. J. S´wia¸tecki, and C. F. Tsang, Ann.Phys. (NY) 105,427 (1977).

[2] V. Y. Denisov, Phys. Lett. B 526, 315 (2002).

[3] R. Bass, Phys. Lett. B 47, 139 (1973); Nucl. Phys. A 231, 45(1974).

[4] P. R. Christensen and A. Winther, Phys. Lett. B 65, 19 (1976).

[5] R. Bass, Phys. Rev. Lett. 39, 265 (1977).

[6] P. M¨oller and J. R. Nix, Nucl. Phys. A 361, 117 (1981).

[7] W. Reisdorf, J. Phys. G: Nucl. Part. Phys. 20, 1297 (1994).

[8] W. D. Myers and W. J. S´wia¸tecki, Phys. Rev. C 62, 044610 (2000).

[9] H. Ngˆo and C. Ngˆo, Nucl. Phys. A 348, 140 (1980).

[10] A. Winther, Nucl. Phys. A 594, 203 (1995).

[11] W. D. Myers and W. J. ´ Swiatecki, Ann. Phys. 55, 395 (1969);Nucl. Phys. A 336, 267 (1980).

[12] C. W. de Jager, H. de Vries, and C. de Vries, At. Data Nucl.Data Tables 14, 479 (1974); H. de Vries, C. W. de Jager, and C. de Vries, *ibid.* 36, 495 (1987)

[13] B. Nerlo-Pomorska and K. Pomorski, Z. Phys. A 348, 169 (1994).

[14] G. Royer and R. Rousseau, Eur. Phys. J. A 42, 541 (2009).

[15]] Ishwar Dutt and Rajeev K. Puri ,Phy. REV. C **81**, 064609 (2010).

CHAPTER 2

2.1 The Dynamical Cluster Decay Model (DCM) For Hot and Rotating Compound Nucleus.

The Dynamical Cluster Decay Model (DCM) [1]-[9] for hot and rotating nuclei (i.e. angular momentum and temperature both not equal to zero) is a reformation of the preformed cluster model of Gupta and collaborators for ground state decay (ℓ =0,t=0)in cluster radioactive (CR)and related phenomena [10]-[18].The DCM is based upon the dynamical (or quantum mechanical) fragmentation theory of cold phenomena in heavy ion reaction and fission dynamics. In DCM, besides the temperature and angular momentum effects in the decay of excited compound nuclei, the deformation and orientation effect of the decay products are also taken care, especially in the decay of heavy excited CN for which the deformation of the decay product seems to play significant role. The DCM, worked out in terms of the collective coordinates of mass asymmetry $\eta=\frac{A_1 - A_2}{A_1 + A_2}$ and relative separation R respectively gives

1. The nucleon-division (or exchange)between the outgoing fragments and
2. The transfer of kinetic energy of incident channel (E_{cm}) to internal excitation (total excitation or total kinetic energy, TXE or TKE) of the outgoing channel. It may be noted that the fixed decay point R = R_a (defined later),at which the process is calculated depends upon temperature T as well as on η (i.e.R(T, η)) .This energy transfer process can be calculated with the help of fig 2.1 .

$$E^*_{CN} = E_{c.m} + Q_{in} = IQ_{out}I + TKE(T) + TXE(T) \quad (2.1)$$

The CN excitation E^*_{CN} is related to temperature T (in MeV) and is given by$E^*_{CN} = \frac{1}{9}AT^2 -$ T(Mev). Using the decoupled approximation to R and η–motions, the DCM define the decay cross section, in terms of partial waves, as [3]-[9]

$$k= \sqrt{\frac{(2\mu Ec.m)}{h^2}}; \sigma = \sum_{l=0}^{lc} \sigma l = \frac{\pi}{k^2}\sum_{l=0}^{lc}(2l+1)PoP \quad (2.2)$$

Where P_o, the preformation probability refers to η-motion and P, the penetrability to the R-motion . Here the complex fragments (both light and heavy fragments) are treated as the dynamical collective mass motion of preformed cluster or fragments through the barrier .The structure information of the CN enters the model via preformation probability P_o (also known as spectroscopic factor) of the fragments given by the solution of stationary Schrödinger

equation in η at the fixed R=R_a, the first turning point of the penetrability path shown in figure 1 for different ℓ -values.

$$\left\{-\frac{\hbar^2}{2\sqrt{B_{\eta\eta}}}\frac{\partial}{\partial\eta}\frac{1}{\sqrt{B_{\eta\eta}}}\frac{\partial}{\partial\eta}+V_R(\eta,T)\right\}\psi^{\nu}(\eta)=E^{\nu}\psi^{\nu}(\eta) \tag{2.3}$$

With ν =0,1,2,3,….referring to the ground state and excited state solution .

For the decay of the hot compound nucleus, we use the postulate of first turning point

$$R_a=R_t+\Delta R(T) \tag{2.4}$$

Where

$$R_t=R_1+R_2 \tag{2.5}$$

ΔR(T) is the neck length parameter that assimilates the neck formation effects. This method is introducing a neck length parameter similar to that used in scission point [21] and saddle point [22],[23]statistical fission model. The R_i are radius vectors which are also made temperature dependent can be calculated as

$$R_i(\alpha_i)=R_{0i}\left[1+\sum_{\lambda}\beta_{\lambda i}Y_{\lambda}^{(0)}(\alpha_i)\right] \tag{2.6}$$

With $R_{0i}(T) = 1.28A_i^{1/3} - 0.76 + 0.8A_i^{-1/3}\times(1 + 0.0007T^2)$, (2.7)

The corresponding potential V (R_a) acts like an effective Q-value, Q_{eff} , for the decay of the hot CN at temperature T, to two exit-channel fragments observed (T=0), defined by

$$Q_{eff}(T) = B(T) - [B_L(T = 0) + B_H(T = 0)$$

$$= TKE(T) = V(R_a(T)) \tag{2.8}$$

With B's as the respective binding energies. The above defined decay of a hot CN into two cold (T=0) fragments, via Eq.(2.8), could apparently be achieved only by emitting some light particle (s)(LPs), like n, p, α, or γ-rays of energy.

By defining Q_{eff} (T) as in Eq. (2.8), in this model we treat the LP emission at par with the heavy fragments, called intermediate mass fragments (IMFs) emission. Thus, in this model a non-statistical dynamical treatment is attempted for not only the emission of IMFs but also of

multiple LPs, understood so-far only as the statistically evaporated particles in a CN emission. It may be reminded here that the statistical model (CN emission) interpretation of IMFs is not as good as it is for the LP production [21–26].

In terms of Q_{eff} (T), the second turning R_b satisfies (fig.1)

$$V(R_a, l) = V(R_b, l) = Q_{eff}(T, l) = TKE(T). \quad (2.9)$$

With the l -dependence of R_a defined by

$$V(Ra, l) = Q_{eff}(T, l = 0), \quad (2.10)$$

which means that the R_a, given by Eq. (2.4), is the same for all l -values, and that V (Ra, l) acts like an effective Q-value, Q_{eff} (T, l), given by the total kinetic energy TKE(T). Then, using (2.9), $R_b(l)$ is given by the l -dependent scattering potentials, at fixed T as

$$V(R, T, l) = V_c(Z_i, \beta_{\lambda i}, \theta_i, T) + V_N(A_i, \beta_{\lambda i}, \theta_i, T) + V_l(R, A_i, \beta_{\lambda i}, \theta_i, T) \quad (2.11)$$

Which is normalized to the exit channel binding energy $B_L(T) + B_H(T)$. Such a potential is illustrated in Fig.1, $^{112}Sn+^{64}Ni \rightarrow ^{178}Pt$, at $\ell = 0$ value.The second turning point R_b is marked for the $\ell = 0\hbar$ case of $R_a = R_t + \Delta R(T)$. The decay path for the l -values begins at $R = R_a$.

The collective fragmentation potential V(R,η,T) in Eq. (2.11) is calculated according to the Strutinsky method by using the T-dependent liquid drop model energy V_{LDM} of [27], with its constants at T=0 refitted [3, 4] to give the recent experimental binding energies given by [28], and again refitted [9] to give the recent experimental binding energies[29] and calculate binding energies[30] (only for those nuclides for which experimental data is not available. the "empirical" shell corrections δU are of Ref. [31]. Then, including the T-dependence also in Coulomb, nuclear interaction potential, and l -dependent potential in complete sticking limit of moment of inertia, we get

$$V(R, \eta, T) = \sum_{i=1}^{2}[V_{LDM}(A_i, Z_i, T) + \sum_{i=1}^{2}[\delta U_i] exp\left(\frac{-T^2}{T_0^2}\right) + V_c(Z_i, \beta_{\lambda i}, \theta_i, T)$$

$$+V_N(A_i, \beta_{\lambda i}, \theta_i, T) + V_l(R, \beta_{\lambda i}+, \theta_i, T) \quad (2.12)$$

2.2 Energy Density Formalism

The energy density formalism defines the nuclear interaction potential as

$$V_N(R) = E(R) - E(\infty) \quad (2.13)$$

i.e. the nucleus-nucleus interaction potential as a function of separation distance, $V_N(R)$, is the difference of the energy expectation value E of the colliding nuclei that are overlapping (at a finite separation distance R) and are completely separated(at R=∞),where

$$E = \int H(\vec{r})d\vec{r} \tag{2.14}$$

with the Skyrme Hamiltonian density

$$\begin{aligned} H(\rho,\tau,J) = {} & \frac{\hbar^2}{2m}\tau + \frac{1}{2}t_0\left[(1+\frac{1}{2}x_0)\rho^2 - (x_0+\frac{1}{2})(\rho_n^2+\rho_p^2)\right] + \frac{1}{12}t_3\rho^{\alpha_0}\left[\left(1+\frac{1}{2}x_3\right)\rho^2 - \left(x_3+\frac{1}{2}\right)\left(\rho_n^2+\rho_p^2\right)\right] \\ & + \frac{1}{4}\left[t_1\left(1+\frac{1}{2}x_1\right) + t_2\left(1+\frac{1}{2}x_2\right)\right]\rho\tau - \frac{1}{4}\left[t_1\left(x_1+\frac{1}{2}\right) - t_2\left(x_2+\frac{1}{2}\right)\right]\left(\rho_n\tau_n + \rho_p\tau_p\right) \\ & + \frac{1}{16}\left[3t_1\left(1+\frac{1}{2}x_1\right) - t_2\left(1+\frac{1}{2}x_2\right)\right]\left(\vec{\nabla}\rho\right)^2 - \frac{1}{16}\left[3t_1\left(x_1+\frac{1}{2}\right) - t_2\left(x_2+\frac{1}{2}\right)\right]\left[\left(\vec{\nabla}\rho_n\right)^2 + \left(\vec{\nabla}\rho_p\right)^2\right] \\ & - \frac{1}{2}W_0(\rho\vec{\nabla}.\vec{J} + \rho_n\vec{\nabla}.\vec{J}_n + \rho_p\vec{\nabla}.\vec{J}_p). \end{aligned} \tag{2.15}$$

Here ρ_q, τ_q and J_q (q=n,p) are the nucleonic, kinetic energy and spin-orbit densities, respectively. m is the nucleon mass. x_i, t_i, α_0 and W_0 are the Skyrme force parameters, fitted by different authors to obtain better descriptions of various ground state properties of nuclei. The Hamiltonian density $H(\vec{r})$ is a function of the nucleus density $\rho(\vec{r})$,kinetic energy density $\tau(\vec{r})$ and spin density $J(\vec{r})$ and these quantities can be obtained from the semiclassical ETF or alternatively from microscopic shell model approaches. The total Hamiltonian density given in Eq. (2.15) is the sum of the spin-orbit density independent Hamiltonian density $H(\rho,\tau)$ and spin-orbit density dependent Hamiltonian density $H(\rho,\vec{J})$.

Then from Eq.(2.13), we get the nuclear interaction potential

$$\begin{aligned} V_N(R) &= \int\left\{H(\rho,\tau,\vec{J}) - \left[H_1\left(\rho_1,\tau_1,\vec{J}_1\right) + H_2\left(\rho_2,\tau_2,\vec{J}_2\right)\right]\right\}d\vec{r} \\ &= V_P(R) + V_J(R) \end{aligned} \tag{2.16}$$

With the spin-orbit density independent part of the interaction potential

$$V_P(R) = \int\left\{H(\rho,\tau) - \left[H_1(\rho_1,\tau_1) + H_2(\rho_2,\tau_2)\right]\right\}d\vec{r} \tag{2.17}$$

And the spin-orbit density dependent interaction potential

$$V_J(R) = \int\left\{H(\rho,\tau) - \left[H_1(\rho_1,\tau_1) + H_2(\rho_2,\tau_2)\right]\right\}d\vec{r} \tag{2.18}$$

Here, $\rho=\rho_1+\rho_2$ and $\vec{J} = \vec{J}_1 + \vec{J}_2$ are for the composite system.

Where $\tau_q(\vec{r})$ is given as,

$$\tau_q(\vec{r}) = \frac{3}{5}(3\pi^2)^{2/3}\rho_q^{5/3} + \frac{1}{36}\frac{\left(\vec{\nabla}\rho_q\right)^2}{\rho_q} + \frac{1}{3}\Delta\rho_q + \frac{1}{6}\frac{\vec{\nabla}\rho_q.\vec{\nabla}f_q + \rho_q\Delta f_q}{f_q} - \frac{1}{12}\rho_q\left(\frac{\vec{\nabla}f_q}{f_q}\right)^2 + \frac{1}{2}\rho_q\left(\frac{2m}{\hbar^2}\right)^2\left(\frac{w_0}{2}\frac{\vec{\nabla}(\rho+\rho_q)}{f_q}\right)^2 \tag{2.19}$$

With f_q as the effective mass form factor,

$$f_q(\vec{r}) = 1 + \frac{2m}{\hbar^2}\frac{1}{4}\left\{t_1\left(1+\frac{x_1}{2}\right) + t_2\left(1+\frac{x_2}{2}\right)\right\}\rho(\vec{r})$$

$$-\frac{2m}{\hbar^2}\frac{1}{4}\left\{t_1\left(x_1+\frac{1}{2}\right) - t_2\left(x_2+\frac{1}{2}\right)\right\}\rho_q(\vec{r})$$

The spin $\vec{J}$ is a purely quantal property, and hence has no contribution in the lowest (TF) order. However, at the ETF level, the second order contribution gives

$$\vec{J}_q(\vec{r}) = -\frac{2m}{\hbar^2}\frac{1}{2}\omega_0\frac{1}{f_q}\rho_q\vec{\nabla}\left(\rho+\rho_q\right) \tag{2.20}$$

For the frozen approximation,

$$\tau(\rho) = \tau_1(\rho_1) + \tau_2(\rho_2),$$
$$\vec{J}(\rho) = \vec{J}_1(\rho_1) + \vec{J}_2(\rho_2), \tag{2.21}$$

With $\rho_i = \rho_{in}+\rho_{ip}$, $\tau_i(\rho_i) = \tau_{in}(\rho_{in})+\tau_{ip}(\rho_{ip})$, and $\vec{J}_i(\rho_i) = \vec{J}_{in}(\rho_{in}) + \vec{J}_{ip}(\rho_{ip})$.

For nuclear density ρ_i, we use the T-dependent Fermi density distribution

$$\rho_i(Z_i) = \rho_{0i}(T)[1+\exp(\frac{Z_i - R_i(T)}{a_i(T)})]^{-1} \tag{2.22}$$

With $Z_2 = R\text{-}Z_1 = [R_1(\alpha_1)+R_2(\alpha_2)+s] - Z_1$, and central density

$$\rho_{0i}(T) = \frac{3A_i}{4\pi R_i^3(T)}\left[1+\frac{\pi^2 a_i^2(T)}{R_i^2(T)}\right]^{-1}$$

with nucleon densities ρ_{iq} further defined as $\rho_{in} = \frac{N_i}{A_i}\rho_i$, $\rho_{ip} = \frac{Z_i}{A_i}\rho_i$, and the half density radii $R_{0i}(T = 0)$ and the surface thickness parameters $a_i(T = 0)$ obtained by fitting the experimental data to the polynomials in nuclear mass A (= 4-209), as [40]

$$R_{0i}\,(T=0) = 0.90106 + 0.10957A_i - 0.0013A_i^2 + 7.71458\times10^{-6}A_i^3 - 1.62164\times10^{-8}A_i^4,$$
$$a_i(T=0) = 0.34175 + 0.01234A_i - 2.1864\times10^{-4}A_i^2 + 1.46388\times10^{-6}A_i^3 - 3.24263\times10^{-9}A_i^4. \tag{2.23}$$

The temperature dependence in the above formulae are then introduced as in Ref. [41],

$$R_{0i}(T) = R_{0i}(T=0)[1+0.0005T^2], \quad a_i(T) = a_i(T=0)[1+0.01T^2]$$

Now, Coulomb potential that describes the force of repulsion between two interacting nuclei due to their charges. It acts along the line joining the two nuclei. The Coulomb potential for two interacting spherical nuclei is given as

$$V_c = Z_1Z_2e^2/R \tag{2.24}$$

For interacting deformed and oriented nuclei, different authors [35]-[39] have derived it differently. In this dissertation work, we have started with Coulomb potential of Wong [38], given for two non-overlapping charge distributions, having quadrupole deformations only, i.e.,

$$V_c = \frac{Z_1 Z_2 e^2}{R} + \left(\frac{9}{20\pi}\right)^{1/2} \left(\frac{Z_1 Z_2 e^2}{R^3}\right) \sum_{i=1}^{2} R_i^2(\alpha_i)\beta_{2i} P_2(\cos\theta_i)$$

$$+ \left(\frac{3}{7\pi}\right)\left(\frac{Z_1 Z_2 e^2}{R^3}\right)\sum_{i=1}^{2} R_i^2(\alpha_i)\left[\beta_{2i} P_2(\cos\theta_i)\right]^2 \qquad (2.25)$$

In this expression, the quadrupole-quadrupole interaction term, proportional to $\beta_{21}\beta_{22}$, is neglected since it has a short-range character. For nuclei lying in the same plane we have generalized it to include the higher order deformations ($\lambda = 3, 4...$), obtaining

$$V_c\left(Z_i, \beta_{\lambda i}, \theta_i, T\right) = \frac{Z_1 Z_2 e^2}{R(T)} 3 Z_1 Z_2 e^2 \sum_{i,i=1,2} \frac{R_i^{\lambda}(\alpha_i, T)}{(2\lambda+1)R(T)^{\lambda+1}} Y_{\lambda}^{(0)}(\theta_i)\left[\beta_{\lambda i} + \beta_{\lambda i}^2 Y_{\lambda}^{(0)}(\theta_i)\right] \qquad (2.26)$$

Now the rotational motion gives an additional energy due to the angular momentum define as

$$V_l\,(R, A_i, \beta_{\lambda i}, \theta_i, T) = \frac{\hbar^2\, l\,(l+1)}{2 I_s(T)} \qquad (2.27)$$

with $I = \mu R^2$, is the non-sticking limit of moment of inertia with as the $\mu = \frac{A1A2}{A1+A2} m$ reduced mass. m is the nucleon mass. In the complete sticking limit, the moment of inertia I is given as,

$$I_s(T) = \mu R^2 + \frac{2}{5} A_1 m R_1^2(\alpha_1, T) + \frac{2}{5} A_2 m R_2^2(\alpha_2, T). \qquad (2.28)$$

However, for the relative separation of interest here, we use the sticking limit. It is relevant to mention here that value of angular momentum extracted experimentally, is based upon moment of inertia limit.

Further, in Eq. (2.26), within the Strutinsky renormalization procedure, we have defined the binding energy B of a nucleus at temperature T as the sum of liquid drop energy $V_{LDM}(T)$ and shell correction $\delta U(T)$ i.e.

$$B(T) = V_{LDM}(T) + \delta U \exp\left(\frac{-T^2}{T_0^2}\right) \qquad (2.29)$$

The T dependent liquid drop part of the binding energy VLDM(T) is from Davidson et al. [27], based on the semi-empirical mass formula of Seeger [32]. For the shell correction δU in

Eq. (2.29), since there is no microscopic shell model known that gives the shell corrections for light nuclei, we use the empirical formula of Myers and Swiatecki [31].

The mass parameters $B_{\eta\eta}(\eta)$, representing the kinetic energy part in Eq. (2.3),are the smooth classical hydro-dynamical masses [33], given by

$$B\eta\,\eta = \frac{AmR2}{4}\left[\frac{vt(1+\gamma)}{vc1+\left(\frac{vt(1+\gamma)}{vc(1+\_\delta 2)}\right)} - 1\right]$$

With $\gamma = = \frac{Rc}{2R}\left[\frac{1}{1+\cos \mathfrak{v}1}\left(1-\frac{Rc}{R1}\right)+\frac{1}{1+\cos \mathfrak{v}\,2}\left(1-\frac{Rc}{R2}\right)\right]$ (2.30)

$\delta = \frac{1}{2R}[(1-\cos \mathfrak{v}_1)+(1-\cos \mathfrak{v}2)]$ (2.31)

and $v_c = \pi^2 R^2{}_c R$

for $\mathfrak{v}_1 = \mathfrak{v}_2 = 0^0$ and R_i taken as temperature dependent.

Finally, the l_c-value in Eq. (2.6) is the critical l-value, in terms of the bombarding energy $E_{c.m.}$ the reduced mass μ and the first turning point R_a of the entrance channel η_{in}, given by

$$l_c = R_a\sqrt{(2\mu[E_{c.m.} - V(R_a, \eta_{in}, l = 0)])}/\hbar \quad (2.32)$$

or, alternatively, it could be fixed for the vanishing of fusion barrier of the incoming channel, called l_{fus}, or else the l-value (l_{max}) where the light-particle cross section $\sigma_{LP} \rightarrow 0$. This, however, could also be taken as a variable parameter [22,34].

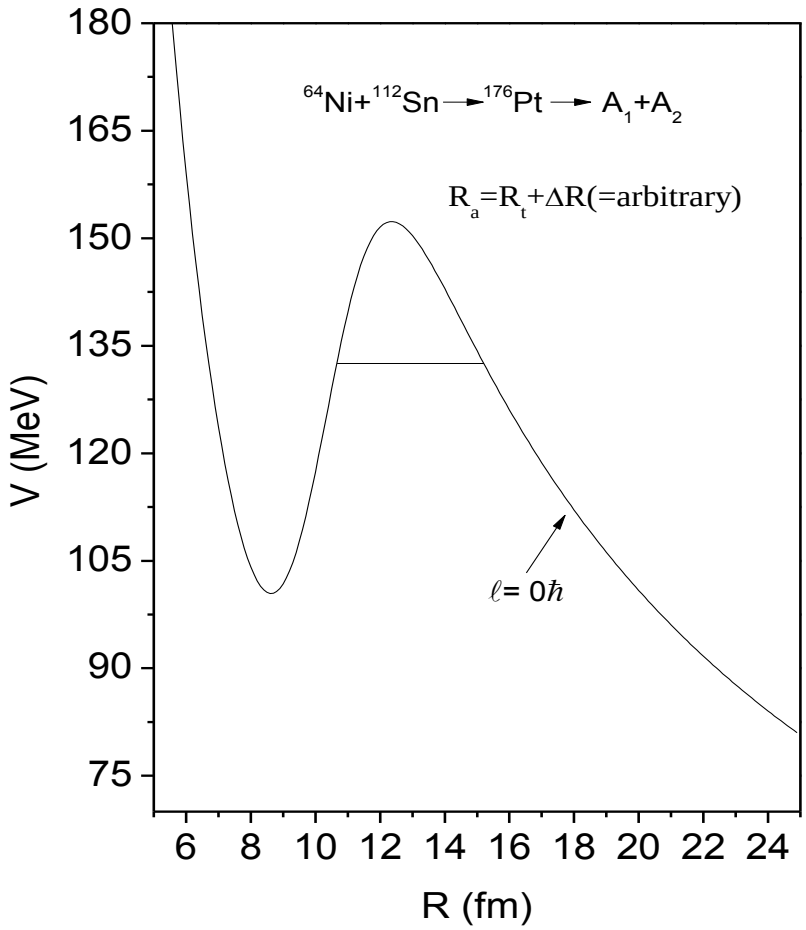

Fig. 2.1 Scattering Plot for $^{64}Ni+^{112}Sn \rightarrow ^{176}Pt \rightarrow A_1+A_2$ reaction.

2.3 WONG FORMULA

After natively Wong formula has also been applied to study the formation process of a compound nuclear system.

According to Wong [51], the fusion cross-section, in terms of angular-momentum ℓ partial waves, for two deformed and oriented nuclei (with orientation angles θ_i), lying in two same planes, and colliding with center-of-mass (c.m.) energy $E_{c.m.}$, is

$$\sigma(E_{c.m.}, \theta_i) = \frac{\pi}{k^2}\sum_{l=0}^{l_{max}}(2l+1)P_l(E_{c.m.}, \theta_i) \quad (2.34)$$

with $k = \sqrt{\frac{2\mu E_{c.m.}}{\hbar^2}}$, and μ as the reduced mass. Here, P_ℓ is the transmission coefficient for each ℓ which describes the penetration of barrier

$V_T^{\ell}(R, E_{c.m.}, \theta_i) = V_N(R, A_i, \beta_{\lambda i}, T, \theta_i) + V_C(R, Zi, \beta_{\lambda i}, T, \theta_i) + V_\ell(R, A_i, \beta_{\lambda i}, T, \theta_i))$, and ℓ_{max} is the maximum angular momentum, defined later. For ℓ=0, total potential V_T is given by,

$$V_T^{\ell=0}(R, E_{c.m.}, \theta_i) = V_N(R, A_i, \beta_{\lambda i}, T, \theta_i) + V_C(R, Zi, \beta_{\lambda i}, T, \theta_i),$$

where nuclear potential V_N is given by

$$\begin{aligned} V_N(R) &= 2\pi\bar{R}\int_{s_0}^{\infty} e(s)ds \\ &= 2\pi\bar{R}\int\left\{H(\rho,\tau,\vec{J}) - \left[H_1(\rho_1,\tau_1,\vec{J}_1) + H_2(\rho_2,\tau_2,\vec{J}_2)\right]\right\}dZ \\ &= 2\pi\bar{R}\int\left\{\left(H(\rho) - \left[H_1(\rho_1) + H_2(\rho_2)\right]\right) + \left(H(\vec{J}) - \left[H_1(\vec{J}_1) + H_2(\vec{J}_2)\right]\right)\right\}dZ \\ &= V_P(R) + V_J(R) \end{aligned}$$

Using Hill-Wheeler [52] approximation of assimilating the shape of the interaction barrier $V_\ell(R, E_{c.m.}, \theta_i)$ through an inverted harmonic oscillator [$V_T^{\ell}(R, E_{c.m.}, \theta_i) = V_B^{\ell}(E_{c.m.}, \theta_i) - \frac{1}{2}\mu\omega^2(R - R_B^{\ell})^2$], the penetrability P_ℓ, in terms of its barrier height $V^{\ell}_B(E_{c.m.}, \theta_i)$ and curvature $\hbar\omega_\ell(E_{c.m.}, \theta_i)$, is

$$P_\ell = [1 + \exp\left(\frac{2\pi(V_B^l(E_{c.m.}, \theta_i) - E_{c.m.})}{\hbar\omega_l(E_{c.m.}, \theta_i)}\right)]^{-1} \quad (2.35)$$

with $\hbar\omega_\ell(E_{c.m.}, \theta_i)$, given as

$$\hbar\omega_l(E_{c.m.}, \theta_i) = \hbar[|d^2V^{\ell}(R)/dR^2|_{R=R^{\ell}_B/\mu}]^{1/2} \quad (2.36)$$

and,the R^{ℓ}_B obtained from the condition

$$|dV_T^{\ell}(R)/dR|_{R=R_B^{\ell}} = 0 \quad (2.37)$$

Instead of solving Eq.(2.28) explicitly, which require the complete ℓ-dependent potentials $V^{\ell}_T(R, E_{c.m.}, \theta_i)$, Wong [51] carried out the ℓ-summation in Eq. (2.34) approximately under the condition:

(i) $\hbar\omega_\ell \approx \hbar\omega_0$, and (ii) $V^\ell{}_B \approx V^0{}_B + \frac{\hbar 2\ell(\ell+1)}{2\mu {R^0}_B{}^2}$,

Which means to assume $R^\ell{}_B \approx R^0{}_B$ also. In other words, both V_B^ℓ and $\hbar\omega_\ell$ are obtained in terms of its ℓ=0 values, with V_B^0 given as the sum of nuclear proximity potential V_P and coulomb potential V_C at $R=R^0{}_B$,

$$V_B^0 = V_P\left(R = R_B^0, A_i, \beta_{\lambda i}, E_{c.m.}, \theta_i\right) + V_C\left(R = R_B^0, Z_i, \beta_{\lambda i}, E_{c.m.}, \theta_i\right)$$

Where $\beta_{\lambda i}$, λ=2,3,4 are the static quadrupole, octupole and hexadecapole deformations.

Using the above two approximations, and replacing the ℓ-summation in Eq. (2.34) by an integral, gives on integration the Wong formula [51]

$$\sigma(E_{c.m.}, \theta_i) = \frac{{R^0}_B^2(\theta_i)\hbar\omega_0(\theta_i)}{2E_{c.m.}} \ln\left[1 + \exp\left\{\frac{2\pi}{\hbar\omega_0(\theta_i)}\left(E_{c.m.} - {V_B}^0(\theta_i)\right)\right\}\right] \tag{2.38}$$

Which on integrating over θ_i gives fusion cross-section,

$$\sigma(E_{c.m.}) = \int_{\theta_i=0}^{\pi/2} \sigma(E_{c.m.}, \theta_i) \sin\theta_1 d\theta_1 \sin\theta_2 d\theta_2 . \tag{2.39}$$

It may be noted that only point of difference between Wong and DCM is that penetrability in Wong formula is calculated by using Hill Wheeler [52] approximation whereas the same in DCM is calculated using WKB approximation. Beside this probability of formation equal to one of fragment at compound nucleus state is taken contrary to DCM approach.

REFERENCES

[1] R.K. Gupta, M. Balasubraniam, C. Mazzocchi, M. La Commara, and W. Scheid, Phys. Rev. C 65, 024601 (2002).

[2] M.K. Sharma, R.K. Gupta, and W. Scheid, J. Phys. G 26, L45 (2000).

[3] R.K. Gupta, R. Kumar, N.K. Dhiman, M. Balasubraniam, W. Scheid, and C. Beck, Phys. Rev. C 68, 014610 (2003).

[4] M. Balasubraniam, R. Kumar, R.K. Gupta, C. Beck, and W. Scheid, J. Phys. G 29, 2703 (2003): R.K. Gupta, M.K. Sharma and B. Singh, Phys. Rev. C-to be published.

[5] R.K. Gupta, M. Balasubraniam, R. Kumar, D. Singh, and C. Beck, Nucl.Phys. A 738, 479c (2004).

[6] R.K. Gupta, M. Balasubramaniam, R. Kumar, D. Singh, C. Beck, and W. Greiner, Phys. Rev. C 71, 014601 (2005).

[7] B.B. Singh, M.K. Sharma, R.K. Gupta, and W.Greiner,Int.J. Mod.Phys.E15, 699 (2006).

[8] R.K. Gupta, M. Balasubraniam, R.Kumar, D.Singh ,S. K. Arun and W.Greiner,J.Phys .G:Nucl.Part. Phys. 32, 345(2006).

[9] B.B. Singh, M.K. Sharma, R.K. Gupta,Phys.Rev. C 77, 054613 (2008).

[10] R.Gupta, in proceedings of the 5th International Conference on Nuclear Research Mechanics, Varenna, 1988, edited by E. gladioli , (Ricerca Scientifica ed Educazione Permanente ,Milano, 1988),p.416.

[11] S.S. Malik and R.K.Gupta, Phys.Rev.C 39, 1992(1989).

[12] R.K.Gupta, W.Scheid, and W.Greiner, J.Phys.G:Nucl. Part. Phys. 17, 1731(1991).

[13] S. Kumar and R.K.Gupta, Phys.Rev. C 49, 1922(1994).

[14] R.K.Gupta and W. Greiner Int. J. Mod. Phys. E 3, 335 (1994, Suppl.).

[15] S. Kumar and R.K.Gupta, Phys. Rev. C 55, 218 (1997).

[16] R.K. Gupta, in Heavy Elements and Related New Phenomena ,edited by W.Greneir and R.K Gupta (World Scientific Singapore) Vol.II ,p.730.

[17] S.K and R.K Gupta ,DAE nucl.Phys.(Sambalpur)52,365(2007).

[18] B.B.Singh,S.K Arun, M.K.Sharma , S.Kanwar and Raj K.Gupta ,DAE Nucl.Phys.(Roorkee), Accepted(2008).

[19] R.K. Gupta, N.Singh, and M. Manhas, Phys. Rev. C 70, 034608 (2004).

[20] R.K. Gupta ,M.balasubramaniam, R.Kumar, N.Singh, M.Manhas, and W. Greiner, J.Phjs. G: Nucl.Part. Phys. C 31, 631(2005).
[21] T. Matsuse, C. Beck, R. Nouicer, and D. Mahboub, Phys. Rev. C 55, 1380 (1997).
[22] S.J. Sanders, D.G. Kovar, B.B. Back, C. Beck, D.J. Henderson, R.V.F. Janssens, T.F. Wang, and B.D. Wilkins, Phys. Rev. C 40, 2091 (1989t).
[23] S.J. Sanders, Phys. Rev. C 44, 2676 (1991).
[24] J. Gomez del Campo, R.L. Auble, J.R. Beene, M.L. Halbert, H.J. Kim, A. D'Onofrio, and J.L. Charvet, Phys. Rev. C 43, 2689 (1991); Phys. Rev. Lett. 61, 290 (1988).
[25] R.J. Charity, M.A. McMahan, G.J. Wozniak, R.J. McDonald, L. G. Moretto, D.G. Sarantites, L.G. Sobotka, G. Guarino, A. Pantaleo, L. Fiore, A. Gobbi and K.D. Hildenbrand, Nucl. Phys. A 483, 371 (1988).
[26] C. Beck, R. Nouicer, D. Disdier, G. Duchˆene, G. de France, R.M. Freeman, F. Haas, A. Hachem, D. Mahboub, V. Rauch, M. Rousseau, S.J. Sanders, and A. Szanto de Toledo, Phys. Rev. C 63, 014607 (2001).
[27] N.J. Davidson, S.S. Hsiao, J. Markram, H.G. Miller, and Y. Tzeng, Nucl. Phys. A 570, 61c (1994).
[28] G. Audi and A.H. Wapstra, Nucl. Phys. A 595, 4 (1995).
[29] G. Audi and A.H. Wapstra and C. Thiboult, Nucl. Phys. A 729, 337(2003).
[30] P. M¨oller, J. R. Nix, W. D. Myers, and W. J. Swiatecki, At. Data Nucl. Data Tables 59, 185 (1995).
[31] W. Myers and W.J. Swiatecki, Nucl. Phys. 81, 1 (1966).
[32] P. A.Seeger, Nucl. Phys. 25, 1 (1961).
[33]H.Kroger and W. Scheid, J. Phys. G 6, L85(1980).
[34] S.J. Sanders, D.G. Kovar, B.B. Back, C. Beck, B.K. Dichter, D. Henderson, R.V.F. Janssens, J.G. Keller, S. Kaufman, T.-F. Wang, B. Wilkins, and F. Videbaek, Phys. Rev. Lett. 59, 2856 (1987).
[35] N. Malhotra and R.K. Gupta, Phys. Rev. C 31, 1179 (1985).
[36] M M¨unchow, D Hahn and W Scheid, Nucl. Phys. A 388, 381 (1982).
[37] M J Rhoades-Brown, V E Oberacker, M Seiwert and W Greiner, Z. Phys. A 310, 287 (1983).
[38] C Y Wong, Phys. Rev. Lett. 31, 766 (1973).

[39] R Aroumougame and R K Gupta, J. Phys. G: 6, L155 (1980).

[49] A. S˘andulescu, R. K. Gupta, W. Scheid and W. Greiner, Phys. Lett. 60B, 225 (1976).

[50] R. K. Gupta, A. S˘andulescu and W. Greiner, Phys. Lett. 67B, 257 (1977);
Rev. Roum. Phys. 23, 51 (1978).

[51] C. Y. Wong, Phys. Rev. Lett. 31, 766 (1973).

[52] D. L. Hill and J. A. Wheeler, Phys. Rev. 89, 1102 (1953); T D Thomas, Phys Rev. 116, 703 (1959).

CHAPTER 3

3.1 Role of Proximity interaction in $^{64}Ni + ^{112,118,124}Sn \rightarrow ^{176,182,188}Pt$.

In this work we planned to see the effective contribution of Proximity interaction in heavy ion collision and related phenomena. The heavy ion collision gives new possibilities to examine the form of ion-ion interaction potential which enables us to investigate the problem related to structure, stability, scattering, decay, multi fragmentation etc. A precise and systematic understanding of the ion-ion interaction between the colliding nuclei is essential in order to have a better insight of a numerous physical phenomena including the universe, working of stars and the abundance of elements available/ anticipated in the universe.

It is well known fact that the Coulomb interaction alone is not enough to describe the formation of a compound nuclear system, beside this the nuclear interaction play a very significant role along with other contributions like angular momentum and deformation dependent interactions. Although the liquid drop energy together with shell correction gives reasonable account of binding strength of a composite nuclear system. But it has been suggested that for ion-ion interactions the contribution of additional Proximity forces is quite essential. The details of these Proximity interactions are given in chapter 1 and 2.

There are various approaches to estimate the ion-ion potential. We have phenomenonological modes like that of Bass [1] who introduce a simple analytical expression for the potential. Then Blocki et al [2] introduced a simple formula for nucleon-nucleon energy as a function of separation between the surfaces of colliding nuclei. This formula is popularly known as pocket formula of Proximity potential. It is relevant to mention that the Proximity potential is free from any adjustment parameter and uses the measured values of surface tension and surface diffuseness. With the availability of data and related development in reference to nuclear interaction, a variety of Proximity formulas have been made available. Such as prox77, prox88, prox00, prox00DP, Bass1973, Bass1977, Bass1980, CW76, BW91, Winther95, Ngo1980, DenisovDP and SEDF based proximity potential. These potential are discussed briefly in chapter 1.

In the present work we propose to see the role of Proximity force in the decay of compound nuclear system formed in heavy ion reactions. We intend to see the effect of different Skyrme forces in reference to Proximity potential used to understand the decay mechanism of heavy nuclear systems within the framework of Dynamical Cluster Decay Model DCM (discussed in chapter 2). As stated earlier DCM, is a versatile model with effects of deformations and

orientations explicitly included and the preformation probability being a handy parameter in reference to nuclear structure information. This effort of testing the role of different Skyrme interactions in the Proximity interactions will certainly be of use to single out the appropriate Skyrme force for the decay mechanism within DCM approach.

3.2 Calculation and results

The decay of ^{176}Pt nuclei is measured over a wide range of centre of mass energies [3,4,5],both below as well as above the Coulomb barrier. We made the Proximity potential calculations to study the decay mechanism of ^{176}Pt by using semi classical Extended Thomas Fermi (ETF) approach in SEDF under frozen approximation.

In figure 3.1 shows the calculated fragmentation potential for $^{64}Ni+^{112}Sn\rightarrow^{176}Pt\rightarrow A_1+A_2$ reaction using dynamical cluster model DCM. It may be noted that proximity potentials within DCM approach is generally calculated using Blocki pocket formula. In the present work we have studied proximity interaction with Blocki as well as EDF based Proximity potential using GSkI [6] and SIII forces.

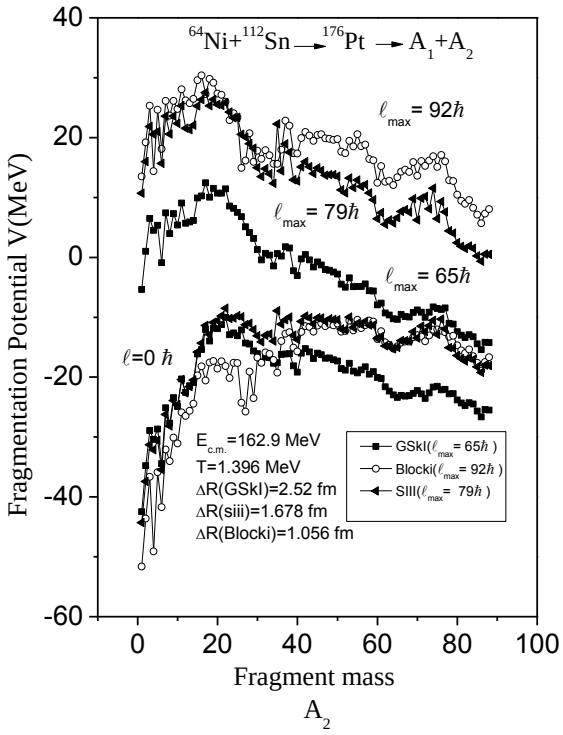

Figure 3.1 Fragmentation potential for the decay of ^{176}Pt nuclei, plotted for ℓ=0 and ℓ_{max} and compare with GSkI ,SIII and Blocki.

From figure 3.1 one may clearly see that behavior of Blocki based fragmentation path is similar to that with SIII Skyrme force. However fragmentation path changes drastically for GSkI force. The interesting aspect of present set of calculation is that the evaporation residue or fission data could be fitted with either with the three chosen Proximity interactions for different value of neck length parameter ΔR, the only parameter of DCM. As the available data could be fitted with either of chosen proximity interaction, so there seems an opportunity to account for comparative behavior of these Proximity interactions in reference to decay of a hot compound nucleus ^{176}Pt formed in ^{64}Ni induced reaction.

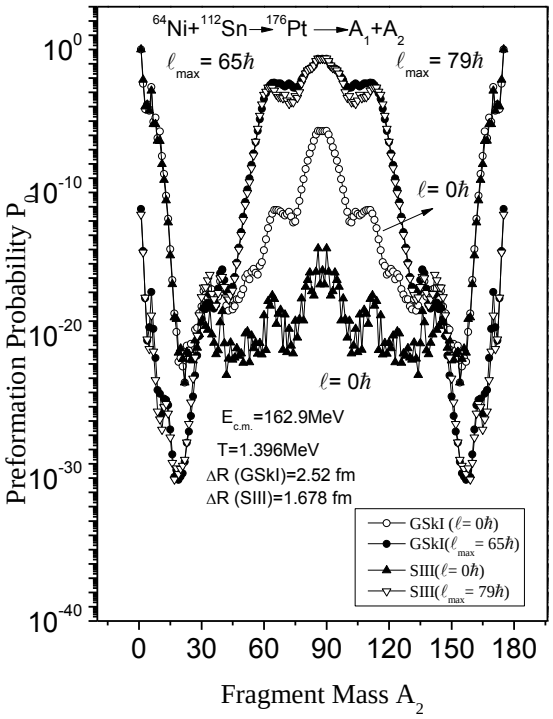

Figure 3.2 Preformation probability P_0 as a function of fragment mass A_2 for $^{176}Pt \rightarrow A_1+A_2$.

In figure 3.2 we have plotted the preformation probability P_0 as function of fragment mass for SIII and GSkI force at two extreme values of angular momentum ℓ. The P_0 for Blocki is not shown, as the behaviour of fragmentation is similar to SIII case as shown in figure 3.1.

Although the fragmentation path is different for SIII based Proximity and Blocki based Proximity at $\ell=0$, the same seems to be quite similar at $\ell=\ell_{max}$. In other words the probability of formation of fragments is similar for GSkI and SIII force at $\ell=\ell_{max}$ where as the same becomes quite different at $\ell=0$. Another interesting aspect to be noted that the symmetric fission seems to be more favourable with either of the Proximity interaction, just in line with [7,8] for blocki case.

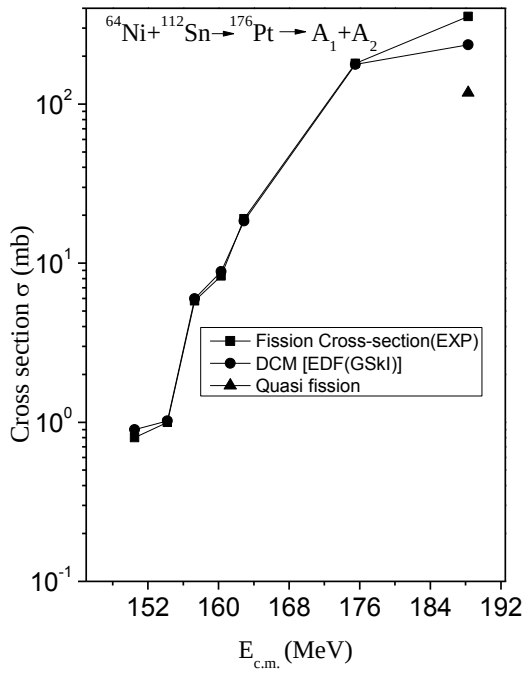

Figure 3.3 Fission cross-section for $^{64}Ni+^{112}Sn\rightarrow^{176}Pt\rightarrow A_1+A_2$ compare with experimental data.

Figure 3.3 gives the comparison of DCM based fission cross-section calculated using GSkI force (in Proximity potential), with experimental data. The available data could be fitted at $E_{c.m.}$ energies except at the highest one where DCM based calculations seems to underestimate experimental data , predicting possibility of Quasi fission component at this highest center of mass energy.

The similar comparison could be worked out with SIII force as well but results are shown only for GSkI force in figure 3.3.

Figure 3.4 shows DCM based evaporation residue cross-section compared with experimental data. A near exact comparison for ER data over a wide range of incident center of mass energy spread on either side of Coulomb barrier, shows the strength and importance of DCM model in reference to problems involving nuclear reaction dynamics at low energy region.

Figure 3.5 gives the neck length parameter ΔR as function of $E_{c..m.}$ (a) for σ_{ER} fitting and (b) for $\sigma_{Fission}$ fitting. One may see that ΔR for fission increases almost linearly with $E_{c..m}$ whereas the same for ER shows similar trend at lower center of mass energies and then stabilizes higher energy region.

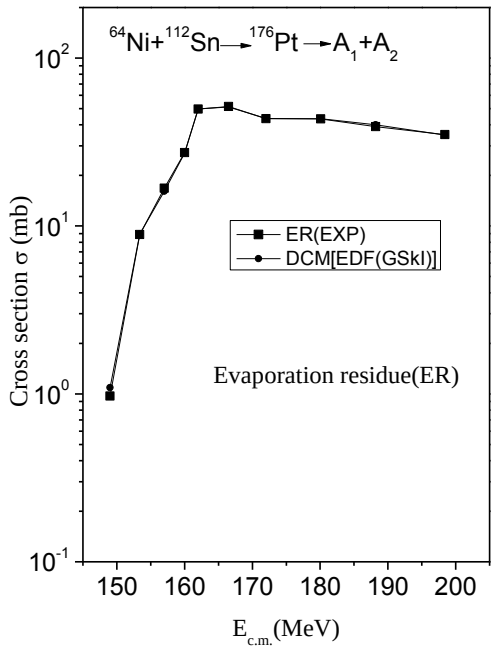

Figure 3.4 DCM based evaporation residue cross section σ_{ER} for $^{64}Ni+^{112}Sn\rightarrow^{176}Pt\rightarrow A_1+A_2$ compared with experimental data.

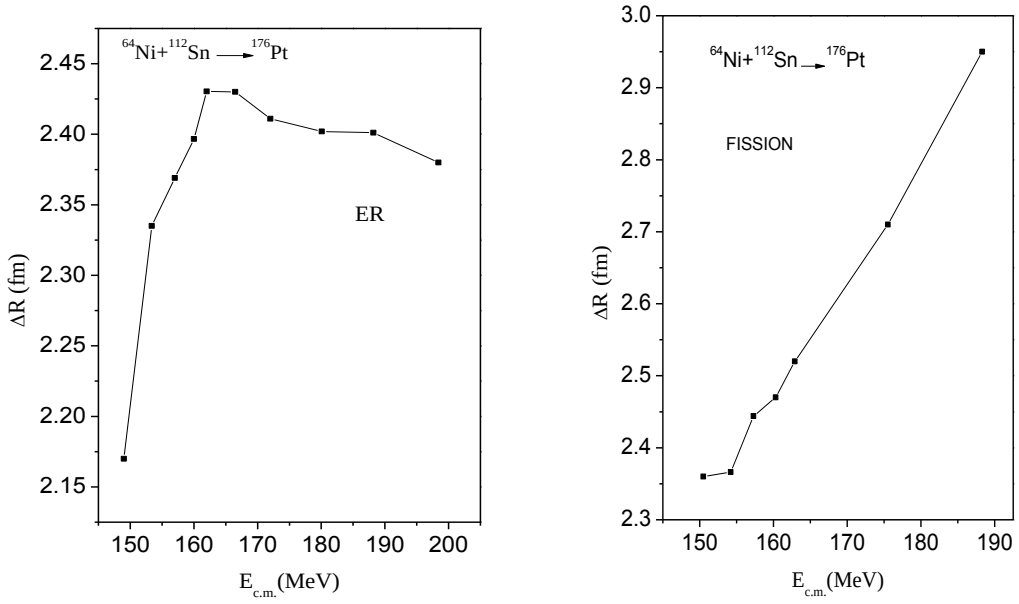

(a) for ER (b) for fusion

Figure3.5 The neck-length parameter ΔR plotted as a function of $E_{c.m.}$for $^{64}Ni+^{112}Sn\rightarrow^{176}Pt\rightarrow A_1+A_2$.

We have also worked on fusion of $^{64}Ni+^{112\text{-}124}Sn$ reaction by fitting the fusion cross sections($\sigma_{ER}+\sigma_{fission}$) over a wide range of center of mass energies using ℓ-summed Wong formula [9].

The wong formula[10] is same as DCM , the only difference is that the penetrability in Wong formula is calculated in the Hill wheeler approximation[11] of inverted harmonic oscillator for the interaction potential of the incoming channel whereas in DCM it is calculated by WKB integral. Beside this the preformation probability is $P_0=1$ in Wong formula. In ref [3,4,5] the data for evaporation residue and fission cross-section is separately available and to get the data for fusion cross-section we have take average value of closely related $E_{c.m.}$ values and then fitted the cross sections by using ℓ-summed Wong formula.

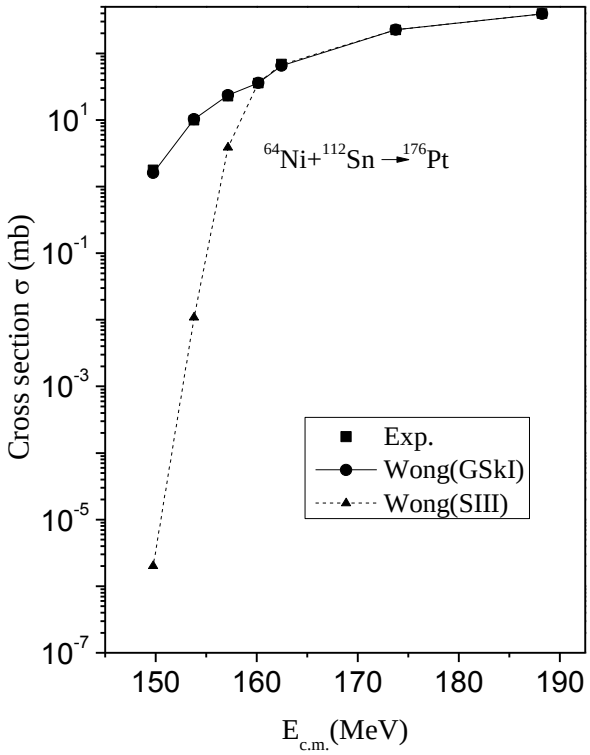

Figure 3.6 The comparison of σ_{fusion} (Wong) with $E_{c.m.}$ using GSkI and SIII forces, compared with averaged experimental data for $^{64}Ni+^{112}Sn \rightarrow ^{176}Pt$.

We notice that in figure 3.6 GSkI force fits the averaged experimental fusion cross-section data nicely. Whereas SIII force needs barrier modification [9] below the Coulomb barrier energies. Although with addition of extra neutrons that is for the reactions $^{64}Ni+^{118\text{-}124}Sn$, the comparison with SIII improve relatively as shown in figures 3.7 & 3.8.

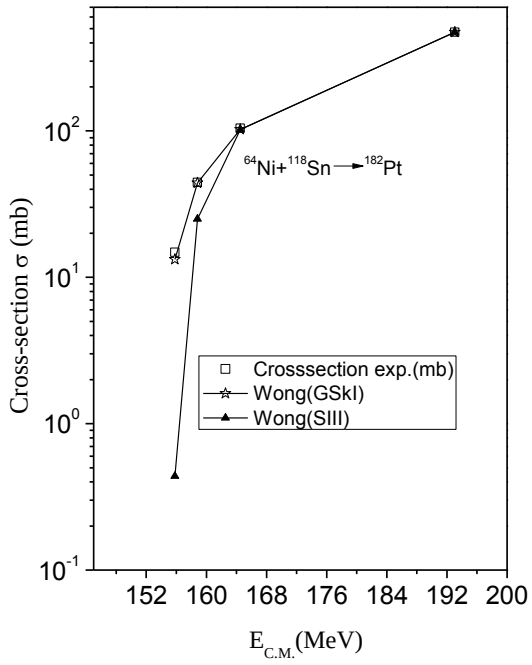

Figure 3.7 The comparison of σ_{fusion} (Wong) with $E_{c.m.}$ using GSkI and SIII forces, compared with averaged experimental data for $^{64}Ni+^{118}Sn\rightarrow^{182}Pt$.

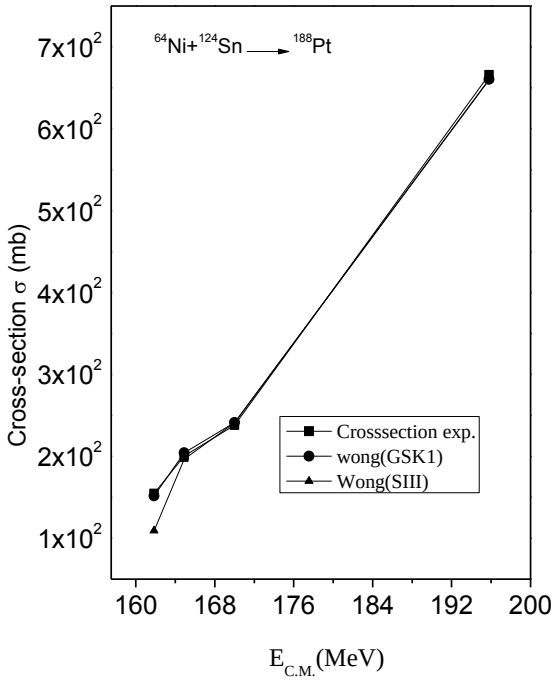

Figure 3.8 The comparison of σ_{fusion} (Wong) with $E_{c.m.}$ using GSkI and SIII forces, compared with averaged experimental data for $^{64}Ni+^{124}Sn\rightarrow^{188}Pt$.

So one may conclude that for ^{64}Ni based reactions only GSkI force fits the fusion experimental data with ℓ-summed Wong formula at below and above the Coulomb barrier. SIII force seems to be fine at higher $E_{c.m.}$ values and for relatively neutron rich cases even at smaller $E_{c.m.}$ values. On the other hand SIII and GSkI seems to complement each other in the frame work of DCM. Whereas SIII based fragmentation is similar to Blocki case and GSkI gives modified fragmentation path. The details of DCM and Wong based calculation cross-section are given in table 3.1 and 3.2 respectively.

Table 3.1(a) Fusion excitation functions for $^{64}Ni+^{112}Sn\rightarrow^{176}Pt$ using ℓ-summed Wong formula using GSkI and SIII force, compared with σ_{fusion}(expt.).

$E_{c.m.}$(MeV)	Cross-section (mb)			ℓ_{max}	
	σ_{exp}	σ_{GSkI}	σ_{SIII}	GSkI	SIII
149.75	1.77	1.6063	0.000002	53	11
153.8	9.90	10.31	.010843	10	36
157.15	22.60	23.58	3.839	14	49
160.15	35.6	36.15	36.47	18	20
162.45	68.70	65.29	67.92	24	25
173.75	223.3	227.05	226.9	47	47
188.25	393.60	391.73	391.22	64	64

Table 3.1(b) Fusion excitation functions for $^{64}Ni+^{118}Sn\rightarrow^{182}Pt$ using ℓ-summed Wong formula using GSkI and SIII force, compared with σ_{fusion}(expt.).

$E_{c.m.}$(MeV)	Cross-section (mb)			ℓ_{max}	
	σ_{exp}	σ_{GSkI}	σ_{SIII}	GSkI	SIII
193.95	473.5	473.34	472.6	71	71
164.5	104.2	102.35	101.96	30	30
158.8	44.5	44.17	25.054	20	53
155.8	14.8	13.23	0.4379	10	44

Table 3.1(c) Fusion excitation functions for $^{64}Ni+^{124}Sn \rightarrow ^{188}Pt$ using ℓ-summed Wong formula using GSkI and SIII force, compared with σ_{fusion}(expt.).

.

$E_{c.m.}$(MeV)	Cross-section (mb)			ℓ_{max}	
	σ_{exp}	σ_{GSkI}	σ_{SIII}	GSkI	SIII
195.8	665.9	660.51	659.89	85	85
170.01	237.9	241.37	240.89	48	48
164.89	200.6	204.19	196.65	43	67
161.85	154.6	151.57	109.04	37	61

Table 3.2 DCM based parameterization for $^{64}Ni+^{112}Sn \rightarrow ^{176}Pt \rightarrow A_1+A_2$. The calculated ER and fission cross-section are compared with experiments (with GSkI force)

$E_{c.m.}$ (MeV)	Cross-section σ_{ER} (mb)		ΔR (fm)	ℓ_{max}	$E_{c.m.}$(MeV)	Cross-section $\sigma_{Fission}$ (mb)		ΔR (fm)	ℓ_{max}
	Exp	DCM				Exp	DCM		
198.4	35	34.8	2.38	68	188.3	354.6	236(fission)+118(Quasi fission) =354	$2.95\sigma_{fiss}/2.8222\ \sigma_{Qf}$	74
188.2	39	40	2.4011	67	175.5	179.7	177.4	2.71	70
180.1	43.4	43.5	2.402	66	162.9	19	18.42	2.52	65
172	43.6	43.7	2.411	65	160.3	8.3	8.84	2.47	64
166.5	51.5	51.2	2.43	64	157.3	5.8	5.98	2.444	63
162	49.7	49.8	2.4303	63	154.2	1	1.02	2.3663	60
160	27.3	27.2	2.3967	62	150.5	0.8	0.9	2.36	59
157	16.8	16.1	2.369	61					
153.4	8.9	8.94	2.335	59					
149	0.97	1.09	2.17	59					

References

[1] R. Bass, Phys. Lett. B 47, 139 (1973); Nucl. Phys. A 231, 45 (1974).

[2] J. Blocki, J. Randrup, W. J. S´wia¸tecki, and C. F. Tsang, Ann. Phys. (NY) 105, 427 (1977).

[3] W S Freeman et al 1983 Phys. Rev. Lett. 50 1563.

[4] K T Jesko et al 1986 phys. Rev. C 34 2155.

[5] J F Liang et al 2007 phys. Rev. C 75 054607.

[6] B. K. Agrawal, S. K. Dhiman, and R. Kumar, Phys. Rev. C. 73, 034319 (2006).

[7] M.K. Sharma, S. Kanwar and R.K. Gupta, AIP Conf. Proc. C P1265 37-41 (2010).

[8] M.K.Sharma, S.Kanwar, G.Sawhney, R.K.Gupta and W.Greiner, J. Phys. G: Nucl. Part. Phys. 38, 055104 (2011).

[9] R. Kumar, M. Bansal, S. K. Arun and R. K. Gupta, Phys. Rev. C 80, 034618 (2009).

[10] C. Y. Wong, Phys. Rev. Lett. 31, 766 (1973).

[11] D. L. Hill and J. A. Wheeler, Phys. Rev. 89, 1102 (1953); T D Thomas, Phys. Rev. 116, 703 (1959).